Functional rerouting via the structural connectome is associated with better recovery after mild TBI

Amy F. Kuceyeski[1,2,†], Keith W. Jamison[1], Julia P. Owen[3], Ashish Raj[3] and Pratik Mukherjee[3,4]

[†]Correspondence to: Amy F. Kuceyeski, Assistant Professor of Mathematics and Neuroscience, Weill Cornell Medicine. Email: amk2012@med.cornell.edu

[1]Department of Radiology and [2]Brain and Mind Research Institute, Weill Cornell Medicine, 407 E. 61 Street, New York, NY 10065, USA

[3]Department of Radiology and Biomedical Imaging and [4]Department of Bioengineering and Therapeutic Sciences, University of California, San Francisco, San Francisco, CA, USA

Short running title: Connectomics in traumatic brain injury

Abstract

Traumatic brain injury damages white matter pathways that connect brain regions, disrupting transmission of electrochemical signals and causing cognitive and emotional dysfunction. Recovery occurs within weeks or months in some individuals, while others suffer chronic and debilitating impairment. The mechanism for how the brain compensates for injury has not been fully characterized. Here, we collect global structural and functional connectome metrics (derived from diffusion and resting-state functional MRI, respectively) and neuropsychological scores in 26 mild traumatic brain injury subjects (29.4±8.0 years of age, 20 male) at 1 month and 6 months post-injury. In addition, we quantified the relationship between functional and structural connectomes using network diffusion model propagation time, a measure that can be interpreted as how much of the structural connectome is being utilized for the spread of functional activation, which is captured via the functional connectome. A measure of overall cognition showed significant improvement from 1 month to 6 months ($t = -2.15$, $p < 0.05$). None of the structural or functional global connectome metrics were significantly different between 1 month and 6 months, or when compared to a group of 34 age- and gender-matched controls (28.6±8.8 years, 25 male). We predicted longitudinal changes in overall cognitive function from changes in global connectome measures using a partial least squares regression model (cross-validated $R^2 = 0.21$). We show that longitudinal increases in network diffusion model propagation time, decreases in structural and functional connectome efficiency, increases in structural connectome characteristic path length and decreases in functional connectome clustering coefficient were significant predictors of longitudinal improvement in cognitive function. We interpret these findings

as support for the "functional rerouting" hypothesis of neuroplasticity after injury, wherein impaired structural connections are compensated for by rerouting of functional connections along alternate, possibly less efficient, structural pathways.

Keywords: concussion, connectome, traumatic brain injury, CNS injury: Imaging, imaging methodology, tractography, cognition, neuroplasticity, resting state connectivity

Abbreviations: traumatic brain injury (TBI), structural connectome (SC), functional connectome (FC), network diffusion (ND), functional MRI (fMRI), diffusion MRI (dMRI), principal component analysis (PCA), partial least squares regression (PLSR), confidence interval (CI), Attention Network Test (ANT), California Verbal Learning Test II (CVLT-II), Coma Recovery Scale – Revised (CRS-R)

1.0 Introduction

Impaired cognitive abilities, including attention and memory, are the most common and debilitating cognitive deficits following traumatic brain injury (TBI) (Ashman *et al.*, 2006; Brenner, 2011; Willmott *et al.*, 2009). More than 5.3 million persons in the US alone are living with TBI-related cognitive dysfunction (Langlois *et al.*, 2006), with an estimated 1.5 million new cases each year, resulting in a total annual medical cost of $77 billion. Recent increases in sports-related and military-related mild TBI have propelled research focus on this disease to the forefront. While both spontaneous and rehabilitation-driven recovery is observed in some individuals after mild TBI (McCrea *et al.*, 2009), between 10-20% of sufferers have persistent cognitive or emotional dysfunction (McAllister *et al.*, 2006; Wood, 2004).

Diffuse axonal injury that occurs in mild TBI can result in neurological impairment by damaging the brain's structural white matter connections, impacting their ability to transmit neuronal signals. Many studies have found relationships between biomarkers of diffuse axonal injury, including diffusion tensor imaging summary statistics such as fractional anisotropy, and cognitive impairment (Kuceyeski *et al.*, 2011; Niogi *et al.*, 2008; Sharp *et al.*, 2014; Yuh *et al.*, 2014). Diffuse axonal injury can also impact network-level measures of structural connectivity (SC) and functional connectivity (FC). Connectomics, a method that enables network-level analysis of anatomical (measured via diffusion MRI) and physiological (measured via functional MRI, magnetoencephalography or EEG) connections between brain regions, has also been applied in mild TBI (Irimia *et al.*, 2012; Sharp *et al.*, 2014; Spielberg *et al.*, 2015). Pandit et al., (2013) found reduced overall FC, longer global characteristic path length and

reduced global efficiency in mild TBI vs. normal controls, while Nakamura et al., (2009) showed lower small world indices in the resting-state FC network. A few publications report improvements in SC related to recovery from severe brain injury (Fernández-Espejo *et al.*, 2011; Sidaros *et al.*, 2008; Voss *et al.*, 2006), although another showed long-term impairment of white matter 5 years post-injury even in those individuals that had recovered (Dinkel *et al.*, 2014). Correlations between network-level improvements in FC and recovery post-injury are more widely reported (Demertzi *et al.*, 2014; Laureys and Schiff, 2012; Sharp *et al.*, 2011; Soddu *et al.*, 2011; Vanhaudenhuyse *et al.*, 2010).

While recovery from TBI depends on both the pattern of damage to the SC network and plasticity of the SC and FC network, few studies analyze the two together (Caeyenberghs *et al.*, 2013, 2017). One study showed TBI patients with more SC injury had less FC in the default mode network (Sharp *et al.*, 2011). Palacios et al., (2013) found increased FC in frontal areas in chronic TBI patients compared to controls, which was also positively correlated with better cognitive outcomes and negatively correlated with SC measures.

While these studies shed light on the relationship between FC, SC and recovery, they are statistical or phenomenological, and do not utilize recent advances in modeling the relationship between FC and SC. Recent work has focused on implementing mathematical models that formalize the relationship between SC and FC in both normal and pathological populations (Cabral *et al.*, 2011; Das *et al.*, 2014; Deco *et al.*, 2012; Fernández Galán, 2008; Honey *et al.*, 2009; Messé *et al.*, 2014; Woolrich and Stephan, 2013). One recent publication in particular mathematically related FC and SC via the Network Diffusion (ND) model (Abdelnour *et al.*, 2014), which assumes functional activation diffuses along white matter connections. This model enables quantification of

the FC-SC relationship via a parameter called ND model propagation time, which is the amount of model time that is needed to "play out" the simulated activation propagation within the SC network to best match the observed FC, i.e. "network depth". ND model propagation time can interpreted as a metric of "distance" between SC and FC; the smaller the distance, the more trivially FC can be explained by SC. Our recent cross-sectional study showed that ND model propagation time was the only global connectome metric (including FC and SC metrics) correlated with Coma Recovery Scale – Revised (CRS-R) after severe brain injury (Kuceyeski *et al.*, 2016). Specifically, increased ND model propagation time was correlated with better level of consciousness as measured by CSR-R, a finding that we also replicated in numerical simulations of injury and recovery. We interpreted the observed relationship between increased ND model propagation time and better recovery as evidence for global cerebral neuroplasticity via "functional rerouting" – i.e. reorganization of functional connectivity to compensate for damaged structural connections. We interpreted higher ND model propagation times in recovery as indicating the existence of intact, less efficient SC pathways that were recruited by the brain for functional reconnection. We conjecture that functional rerouting is especially important in the case of severe brain injury where there is a lower chance of repairing impaired structural connections. In cases of more mild injury, as in the patient population in this study, we hypothesize that there may be, in addition to functional rerouting, a "functional reconnection" mechanism that entails reestablishment of functional connections via the original, mildly impaired white matter pathway. The ND model parameter would also increase in the case of functional reconnection as activation would be propagating along a weaker SC pathway, resulting in the need for increased ND model

propagation time to recapitulate the observed, re-established FC along an impaired SC (see Fig 1). Therefore, in this work, we test the functional rerouting/reconnection hypothesis by examining if longitudinal increases in ND model propagation time are associated with better cognitive recovery in mild TBI patients, using tests of attention and memory.

2.0 Materials and Methods

2.1 Data

Data from 51 subjects (29.6±8.6 years of age, 35 male) that incurred mild TBI was collected at 1 week, 1 month, 6 months and 12 months post-injury. Our hypothesis is that most recovery occurs between the 1 month and 6 month time points (Losoi *et al.*, 2016), so we chose to focus on the data from those two time points only. A total of 27 subjects had complete datasets (neuropsychological test scores and MRI data) from both 1 and 6 months (29.1±8.1 years of age, 21 male). The conditions for inclusion were blunt, isolated mild TBI, defined as Glasgow Coma Scale of 13–15 at injury, loss of consciousness less than 30 minutes and post-traumatic amnesia less than 24 hours. No imaging was used to define mild TBI. The conditions for exclusion were pregnancy or other contraindication to MRI, a history of neurological/psychiatric diagnosis, prior seizure, or drug/alcohol abuse. MRIs were collected on a 3T GE Signa EXCITE scanner and included structural scans (FSPGR T1, 1x1x1 mm^3 voxels), resting-state fMRI (7 min, 3.4x3.4x4.0 mm^3 voxels, 2 sec sampling rate) and 55-direction high angular resolution diffusion MRI (dMRI: b=1000 sec/mm^2, 1.8x1.8x1.8 mm voxels). Neuropsychological testing of attention and learning/memory consisted of 9 subscores within the Attention

Network Test (ANT) (Fan *et al.*, 2002), as well as 16 subscores of the California Verbal Learning Test-II (CVLT-II) (Jacobs and Donders, 2007), including measures of short delay/long delay/free/cued recall and total intrusions/repetitions/recognition. The same MRI sequences were acquired in 34 age- and gender-matched normal controls (28.6±8.8 years, 25 male) for comparison.

2.2 Image Processing

Gray matter and white matter tissues were classified and the gray matter further parcellated into 86 anatomical regions of interest using the semi-automated FreeSurfer software (Fischl and Dale, 2000). Cortical and subcortical parcellations were then used in the construction of the SC and FC networks.

2.2.1 Extraction of the functional connectomes

All data were analyzed in Matlab using SPM12 and the CONN functional connectivity toolbox 17f (http://www.nitrc.org/projects/conn) (Whitfield-Gabrieli and Nieto-Castanon, 2012). Preprocessing of the fMRI data was performed using the CONN toolbox "Direct normalization to MNI-space" pipeline, which includes motion-correction (simultaneous re-alignment and unwarping), slice-timing correction, and coregistration/normalization to MNI space (3mm voxels). Outlier volumes were removed automatically using the Artifact Detection Tools within the CONN toolbox. The toolbox performs a rigorous regression of head motion (24 total motion covariates: 6 motion parameters plus temporal derivatives and squared terms) and physiological artifacts (10 total CompCor eigenvariates: 5 each from eroded WM and CSF masks (Behzadi *et al.*, 2007)). Notably, this denoising does not regress out global signal, allowing for interpretation of anti-correlations (Chai *et al.*, 2012). Band-pass filtering (0.008-0.09 Hz)

of the residual blood oxygen level-dependent contrast signal was also conducted. Each subject's cortical and subcortical parcellation from FreeSurfer was coregistered and transformed into MNI space, and these parcels were used to extract average functional time series for each anatomical region of interest. The pairwise FC between two regions was defined as the Pearson correlation coefficient between these time-dependent regional signal averages after removing the first five volumes. Correlation coefficients with a corrected p-value of greater than 0.05 were set to zero. Correction for multiple comparisons was performed for each individual using the linear step-up procedure for false discovery rate correction introduced in (Benjamini and Hochberg, 1995).

2.2.2 Extraction of the structural connectomes

Diffusion MRIs were linearly motion corrected using a modified version of FSL's eddy_correct and the linear correction applied to the gradient directions. The dMRIs were then corrected for eddy currents using FSL's eddy_correct. Orientation distribution functions were constructed using FSL's bedpostx (2 fiber orientations, 1000 sample burn in), gray/white matter masks linearly transformed to dMRI space and streamline tractography performed from each voxel in the gray matter/white matter interface (linear interpolation, Euler tracking, step size = 0.625, threshold for fractional anisotropy > 0.15, curve threshold = 70, curve interval = 2). SC matrices were calculated as the number of streamlines connecting any given pair of regions.

2.3 Global Connectome Metrics

Global metrics of average degree, characteristic path length, efficiency, clustering coefficient, modularity and small-world index were calculated for the weighted SC and FC networks using the Brain Connectivity Toolbox (Rubinov and Sporns, 2010). The FC

matrices were converted to absolute values and divided by the mean value for inter-subject normalization. Average node degree of the FC was calculated using the un-normalized version of the FC. Each edge in the SC matrices was divided by the sum of the volumes of the two regions, allowing correction for different sized regions that would have proportionally more/fewer number of seeds in the tractography algorithm. It also adjusts the patient SC to account for any damage-related atrophy in the gray matter regions, allowing for better comparison of graph theoretical measures, since the normalized connection strength is a measure of amount of connectivity proportional to the amount of gray matter that remains. Small-world index *s* was calculated as

$$s = \frac{c/\bar{c}_{rand}}{p/\bar{p}_{rand}}$$

where c and p are the clustering coefficient and characteristic path length of the individual's network. The variables $\bar{c}_{rand}$ and $\bar{p}_{rand}$ are the mean of the clustering coefficient and characteristic path length values of 100 different matrices, each obtained by randomly permuting the original connectivity network's edges 10 times while preserving degree distribution.

2.4 Network Diffusion Model Propagation Time

The network diffusion model, detailed in Abdelnour *et al.*, (2014), relates FC to SC by assuming that neuronal activity (functional activation) diffuses within the SC network. In other words, functional activation is modeled as a random walk within the SC network. Therefore, the rate of change of activation at any node *i*, denoted x_i, is related to the difference between the level of activation at that node and its connected neighbors, relative to the sum of outgoing connections of each node (node degree). That is,

$$\frac{dx_i(t)}{dt} = \frac{\beta}{\sqrt{\delta_i}} \sum_j c_{ij} \frac{1}{\sqrt{\delta_j}} x_j(t) - x_i(t) \quad (1)$$

where the coefficients c_{ij} are the elements of the SC matrix C, $\delta_i = \sum_j c_{ij}$ is the degree of node *i* and β is the rate constant of the exponential decay. This relationship is extended to the entire brain network $\boldsymbol{x}(t)$

$$\frac{dx(t)}{dt} = -\beta \mathcal{L} \boldsymbol{x}(t) \quad (2)$$

where $\mathcal{L}$ is the well-known network Laplacian. The network Laplacian can have different formulations depending on the normalization factor. We choose, as in Abdelnour *et al.*, (2014) and Kuceyeski *et al.*, (2016), to normalize by node degree, resulting in the Laplacian $\mathcal{L} = I - \Delta^{-1/2} \mathrm{C} \Delta^{-1/2}$, where Δ is the diagonal matrix with entries δ_i. We chose to normalize by node degree in order to control for different sized regions in the gray matter parcellation. Therefore, the matrix C in the calculation of the Laplacian is the SC matrix based on streamline count. For any initial configuration, or activation pattern, $\boldsymbol{x_0}$, the solution to Eq (2) is:

$$\boldsymbol{x}(t) = \exp(-\beta \mathcal{L} t) \boldsymbol{x_0} \quad (3)$$

Let A be the observed FC network and $\widehat{\mathrm{A}}$ be the predicted FC network from the ND model. We define the estimated FC of region *i* with all other regions at time *t* as the evolution on the graph of an initial configuration involving only region *i*, i.e. $\hat{a}_i(t) = \exp(-\beta \mathcal{L} t) \mathrm{e}_i$ where e_i is the unit vector in the *i*th direction. If we collect all regions/unit vectors together, we obtain $\langle \hat{a}_1(t) | \cdots | \hat{a}_1(t) \rangle = \exp(-\beta \mathcal{L} t) \langle \mathrm{e}_1 | \cdots | \mathrm{e}_N \rangle$, or

$$\widehat{\mathrm{A}}(t) = \exp(-\beta \mathcal{L} t) \quad (4)$$

which gives the prediction for the observed FC matrix A. The accuracy of this prediction depends on t and β. We do not have an empirical value for β, so we absorb it into the

estimation (by setting it to 1) and allowing t to vary. The special cases $\hat{A}(0) = \boldsymbol{I}$ and $\hat{A}(\infty) = D$, where $D = u_0 u_0^T$ is the steady state solution (outer product of the eigenvector of $\mathcal{L}$ that has a corresponding eigenvalue of 0). Between those cases, a range of functional networks exists. The t that gives the most accurate predicted FC compared to the subject's observed FC is called *ND model propagation time*, denoted t_m. Specifically, ND model propagation time is the t that maximizes

$$c(t) = \frac{cov(A, \hat{A}(t))}{\sigma_A \sigma_{\hat{A}(t)}} \quad (5)$$

Here A and $\hat{A}$ are vectorized versions of the matrices after excluding values on the diagonal. In summary, this procedure uses the ND model to estimate an individual's FC from their SC and then identifies the t that gives the best agreement between the predicted and observed FC, which we call model propagation time. We understand model propagation time, which is unit-less and not related to actual time, as the measure of how much of the SC network is being used for the spread of functional activation as captured with the observed FC network.

2.5 Statistical Analysis

Changes in network metrics from 1 month to 6 months in the mild TBI patients were calculated using a two-tailed, paired t-test (degrees of freedom = 25), while differences between mild TBI (at both 1 month and 6 months) and healthy controls were assessed using an un-paired t-test (degrees of freedom = 58). QQ-plots of the connectome measures were used to verify normality of the connectome measures. P-values for all three sets of t-tests were corrected for multiple comparisons using Benjamini-Hochberg false discovery rate correction and assessed for significance using a threshold of α=0.05. Pearson's correlation was calculated between the FC and SC at 1 month and 6 months,

and between the change in network metrics between 1 and 6 months to evaluate the evolving relationship of FC and SC network metrics (degrees of freedom = 25). Two-tailed p-values were again Benjamini-Hochberg false discovery rate corrected and assessed for significance using a threshold of α=0.05.

For analysis of the relationship between recovery and connectome measures, we first used Principal Components Analysis (PCA) on the 25 subscores of attention (from ANT) and memory/learning (CVLT-II) over all 27 subjects' data from one and 6 months. The first principal component was calculated and taken to be a measure of overall cognition; differences between this measure at 1 and 6 months were compared using a two-tailed, paired t-test (degrees of freedom = 25) and assessed with a significance level of α=0.05. Once an overall measure of recovery was identified, Partial Least Squares Regression (PLSR), a regression technique that can accommodate correlated input variables, was used to model the relationship between changes in global connectome measures and changes in overall cognitive function. Specifically, we estimated change in overall cognitive recovery ($\Delta PCA = PCA_{FU} - PCA_{BL}$) from the various demographics and connectome metrics. The input variables included in the model were those of age, gender, change in ND model propagation time and change in the FC and SC global network metrics of average node degree, characteristic path length, efficiency, clustering coefficient and modularity ($\Delta m = m_{FU} - m_{BL}$) that had trends for correlations ($p<0.10$ uncorrected) with the change in overall cognition. We performed this step as to not include any variables that were clearly not related to change in overall cognition. We used a nested cross-validation procedure to select and fit the models and perform predictions. The outer loop consisted of leave-one-out cross validation; each observation

was held out in turn and the following procedure performed on the remaining training data to select and fit the model. First, the number of components in the PLSR model was chosen as the one that most frequently minimized the Predicted Residual Sum of Squares (Krishnan *et al.*, 2011), calculated via k-fold (k=5) cross-validation with 50 Monte Carlo repetitions, over 1000 bootstrapped samples. Once the optimal number of components was identified, bootstrapping was again employed (with 10000 resamples) using the entire training data set to calculate the regression coefficients and the bias corrected and accelerated 95% confidence intervals (Efron, 1987). The mean of the regression coefficients over the bootstrapped samples was then used to make a prediction for the single set of hold out test data.

3.0 Results

3.1 Post-mild TBI Cognitive Recovery

Fig. 1 shows the first PCA component's coefficients for the 9 subscores of the ANT and the 16 subscores (standardized) of the CVLT-II over the 27 subjects' data from one and 6 months. The first PCA component explained 48% of the variance, while the second and third components explained only 16% and 8%, respectively. The red bars signify that lower scores on that sub-test indicate better function while blue bars signify that higher scores on that sub-test indicate better function. All of the red bars have negative PCA coefficients (except for CVLT-II "repetitions", which has a relatively small positive coefficient) and all blue bars are positive. This indicates that positive values of the PCA component indicate better cognitive scores, and increases over time indicate improvements in cognition. A paired t-test showed a significant increase in the PCA

measure of overall cognition from one to 6 months ($t = -2.15$, $p = 0.04$), see Fig. 3. In a secondary analysis (Supplementary Analysis S1), we included all available neuropsychological data from all time points and re-performed the PCA analysis (see Supplementary Fig. 1), which was almost identical to the PCA results in Fig. 2. Supplementary Fig. 2 also shows violin plots of overall cognition from 1 week to 1 month and 6 months to 12 months, neither of which showed significant changes over time, supporting our hypothesis that most recovery would occur between 1 month and 6 months.

3.2 Global network metrics and predicting longitudinal recovery

One subject had an improvement in cognitive function between 1 and 6 months that was more than 1.5 times the inter-quartile range above the third quartile and therefore was excluded from the analyses. The final 26 mild TBI patients with data from 1 and 6 months had demographics (29.4±8.0 years of age, 20 male) that were not significantly different than the entire mild TBI population or the control group. There were no significant differences in any of the global SC and FC network metrics from 1 to 6 months and no significant differences at either time point when compared to healthy controls ($p > 0.05$, corrected for all t-tests), see Supplementary Table 1 for details. Correlations between demographics, change in graph network metrics and change in overall cognition are listed in Supplementary Table 2. The variables that showed trends for a relationship with change in cognition (uncorrected $p<0.10$) were change in ND model propagation time, change in SC characteristic path length, change in SC efficiency, change in SC small-worldness, change in FC efficiency, change in FC characteristic path length and change in FC clustering coefficient. These variables were

then used as inputs to the PLSR models. All 26 PLSR models (over the leave-one-out cross-validation outer loop) included one component only. The predicted values versus observed values are provided in Fig. 4 (hold-out $R^2 = 0.21$). Because we had one PLSR model for each of the leave-one-out iterations (which itself is the mean over the 10000 bootstrapped samples), we report the mean regression coefficient over all 26 models and list the number of times the confidence interval for the regression coefficient did not include 0 in Table 1. We also provide violin plots of the regression coefficients for each input variable over the PLSR models in Fig. 5. Regression coefficients were considered important predictors if their 95% CI did not contain zero in a majority of the 26 leave-one-out models, and are indicated as bold lines in Table 1 and colored violin plots in Fig. 5. Important predictors of better overall cognitive recovery included increased ND model propagation time and SC characteristic path length, decreased SC efficiency, SC small-worldness, FC network efficiency and FC clustering coefficient.

	Mean PLSR Coefficient	Number of times the 95% CI did not include 0 (out of 26)
Δ ND model propagation time	**0.14**	**22**
Δ SC characteristic path length	**0.14**	**25**
Δ SC efficiency	**-0.15**	**26**
Δ SC Small-world metric	-0.14	11
Δ FC efficiency	**-0.11**	**14**
Δ FC clustering coefficient	**-0.12**	**22**
Δ FC modularity	-0.10	2

Table 1: The mean of the PLSR coefficients over the 26 leave-one-out models predicting change in overall cognitive recovery from 1 month to 6 months post-mild TBI. The second column lists the number of times the 95% confidence interval (calculated via the bias corrected and accelerated method) for the PLSR coefficients over the bootstrapped samples did not include zero (out of 26). Bold text indicates those variables whose 95%

CI did not include zero for the majority of the models. Longitudinal changes in both the input and outcome variables were calculated as follow-up minus baseline, so positive coefficients indicate increases in that variable were related to better recovery while negative coefficients indicate decreases in that variable were related to better recovery. Abbreviations: partial least squares regression (PLSR), confidence interval (CI), network diffusion (ND), structural connectome (SC), functional connectome (FC)

4.0 Discussion

We did not detect any significant FC or SC network metric differences between mild TBI and healthy control groups, or any significant changes from 1 month to 6 months within the mild TBI group. However, we observe that increases from 1 month to 6 months post-injury in network diffusion model propagation time, our measure of the relationship between FC and SC, was one of the significant predictors of improvements in overall cognitive function. ND model propagation time can be interpreted as a measure of the amount of SC that is utilized for the spread of functional activation that is captured via the FC network. The model coefficient was positive, indicating that increases in this value were associated with more improvement in cognitive functioning, thus providing support for our functional rerouting/reconnection hypothesis. In functional rerouting, the utilization of less efficient SC pathways for reestablishing FC would result in increased ND model propagation time to allow the functional activation to fully diffuse along the less efficient SC pathways and match the observed FC. We also observed that decreases in SC and FC efficiency and increases in SC characteristic path length were related to better cognitive improvements. These relationships can also be interpreted in the context

of our functional rerouting hypothesis in that less efficient pathways are being utilized for functional reconnection, which would result in decreased efficiency in the FC. The change in SC measures may reflect a strengthening of the less efficient white matter pathways that are being utilized for functional rerouting.

In mild TBI, where white matter injury is less extensive than in moderate or severe TBI, regions with impaired SC may be able to reestablish FC through the original, still impaired white matter connection. This would again result in increased ND model propagation time, as longer model time would be required to allow functional activation to propagate along the impaired structural connection to levels that match the observed functional connection. We conjecture that whether rerouting or reconnection, or a combination of both, is taking place is a function of the level of structural impairment – the more structural impairment the more likely functional rerouting and not reconnection is the primary mechanism for reorganization. Future longitudinal studies with many more subjects will be required to test these hypotheses on a regional level.

Studies that have investigated global network metrics in mild TBI have found mixed results (see Caeyenberghs et al., [2017] for a review), probably due in part to the heterogeneity of the disorder and the populations studied in addition to the complicated relationship between FC/SC and impairment and recovery. Many studies have found no group-wise differences when comparing mild TBI and healthy controls' global network metrics or when comparing longitudinal changes in the mild TBI group (Hillary *et al.*, 2014; Harm Jan van der Horn *et al.*, 2017), which agree with our findings here. While van der Horn et al., [2017b] found no differences in SC global network metrics between TBI and controls, lower global and mean local efficiency were found in the SC networks

of TBI patients without post-traumatic complaints when compared to those with post-traumatic complaints, which is the cross-sectional analog of our longitudinal result that decreased SC efficiency over time was related to better cognitive recovery. The authors also found that lower SC clustering coefficient had a non-significant trend of correlating with higher processing speed cross-sectionally, which we did not find in our longitudinal study. In contrast, other studies have found group-wise differences between mild TBI and healthy controls' global network measures. For example, Pandit et al. [2013] found reduced overall FC, longer characteristic path lengths and reduced efficiency in mild TBI patients versus controls, while Nakamura et al., [2009] showed lower small world indices in the resting-state FC network. Another study showed that moderate to severe TBI patients had lower global SC network efficiency than normal controls and that lower global efficiency was also correlated with worse scores on an executive function task (Caeyenberghs *et al.*, 2014). The discrepancy between their findings and our results could be due to the difference in populations, i.e. moderate to severe versus mild TBI. Kim et al., [2014] showed no differences in transitivity and modularity between mild TBI and controls, but showed longer SC characteristic path lengths were moderately correlated with worse performance on executive function and verbal learning tasks in the mild TBI group. However, multiple comparisons corrections were not performed in this cross-sectional, preliminary study.

Only a few studies have investigated the interplay between FC and SC changes in recovery after mild TBI. One such study showed TBI patients with more SC injury had less FC in the default mode network (Sharp *et al.*, 2011). They also showed that higher resting-state FC in the posterior cingulate cortex was correlated with more efficient

response speeds. Another analysis of task-based FC and SC networks in mild TBI showed that there were no correlations between FC and SC network metrics, no differences in the SC network metrics and significant increases in FC strength in patients versus controls (Caeyenberghs *et al.*, 2013). In another study of chronic TBI patients, Palacios et al., [2013] found increases in FC in frontal areas compared to controls that was positively associated with better cognitive outcomes and negatively associated with a measure of SC. They concluded that altered SC between brain regions could be partly compensated for by increased FC. This conclusion from cross-sectional data is compatible with our current findings of longitudinal increases in ND model propagation and decreases in FC efficiency in recovery. Although younger age in TBI patients has previously been correlated with better recovery (Hukkelhoven *et al.*, 2003; Marquez de la Plata *et al.*, 2008), we did not observe a relationship between age and cognitive recovery in this cohort (Table S2). We conjecture that our data did not show that relationship because our patients were of relatively homogeneous, young age and their injury mild.

In a post-hoc analysis we investigated the Pearson's correlations between the longitudinal changes in all of the SC and FC network metrics, see Supplementary Fig. 3. We see significant (uncorrected $p < 0.05$), moderate correlations between ND model propagation time and change in SC characteristic path length ($r = 0.44$), change in SC efficiency ($r = -0.42$), change in SC clustering coefficient ($r = -0.42$), change in FC degree ($r = 0.40$), change in FC characteristic path length ($r = 0.39$) and change in FC efficiency ($r = -0.41$). This implies that increases in ND model propagation time from 1 to 6 months were related to increases in both SC and FC characteristic path length, increases in FC degree and decreases in FC and SC efficiency. These observations are in accordance with our

functional rerouting hypothesis wherein functional activation is routed along less efficient SC pathways, increasing FC characteristic path length and decreasing FC efficiency, which may in turn strengthen the less efficient white matter pathways, increasing SC path length and decreasing SC efficiency. We also observed that decreases in SC degree over time are correlated to increases in FC degree ($r = -0.39$) and increases in FC characteristic path length ($r = -0.40$).

To our knowledge, this study is one of the first to quantify the longitudinal relationship between the functional and structural connectomes in the context of global cerebral reorganization after traumatic brain injury. Our recent publication (Kuceyeski *et al.*, 2016) performed cross-sectional analyses in severe brain injury patients to show that ND model propagation time was positively correlated with better measures of recovery of consciousness while other global measures of FC and SC were not. As compared to our current study, our previous study was 1) cross-sectional (here we investigated longitudinal relationships), 2) in patients with varying etiology (here we have only mild TBI), 3) in patients with severe injury (here we have mild injury only) and 4) based on Coma Recovery Scale-Revised (here we use cognitive measures ANT/CVLT-II that are sensitive to much lesser degrees of brain dysfunction). Yet, we still observe that ND model propagation time increases with measures of recovery. This robust finding lends confidence that our observations are not a result of chance and that ND model propagation time is indeed capturing some mechanism of global network-level neuroplasticity that is related to recovery after injury.

In our previous paper, we also simulated injury and post-injury recovery using healthy connectomes to explore the impact of these mechanisms on ND model propagation time.

We simulated injury by removing random entries in the SC network and reducing the magnitude of FC in those same entries by a varying percent (25-100%). We simulated recovery by removing random entries in the SC and leaving the FC of those region-pairs intact. Using these simulated networks, we showed that ND model propagation time had decreases in injury and increases in recovery that were proportional to the amount of injury and recovery (see Fig 6 of Kuceyeski *et al.*, 2016), which supported our functional rerouting hypothesis. We conjecture that in the current patient population of mild TBI, there may be some white matter connections that remain impaired and others that can recover. In this case, it is likely that functional rerouting is partially contributing to recovery, with functional reconnection also playing a role.

4.1 Limitations

A limitation of the current work is the relatively small sample size. To combat the effects of the small sample size, we performed leave-one-out cross-validation and bootstrapping for model selection and inference. There are also some limitations in the data processing. We did not have fieldmaps with which to perform EPI distortion correction for dMRI. However, the degree of anatomical distortion was low in this data due to relatively strong gradients with a short TE of 63 ms, as well as the high spatial resolution of 1.8-mm isotropic voxels. Tractography algorithms have issues reconstructing fibers that are crossing and kissing – here we use multi-tensor fitting of the dMRI to minimize this issue.

Previous studies in mild TBI have shown correlations between attention, memory and depression measures and connectivity metrics in particular brain regions (Bonnelle *et al.*, 2011; Hampson *et al.*, 2006; Harm J. van der Horn *et al.*, 2017; Sharp *et al.*, 2011). We

focused here on global connectomic measures since our sample size was not large and we wanted to minimize the effect of heterogeneity of injury patterns and reduce the number of statistical tests/input variables. We believe global network metrics would be more robust to the heterogeneity in patient injury patterns and the global nature of diffuse axonal injury. We believe that investigating functional rerouting on a regional basis would be an excellent area of research, and we plan to do this with larger sets of data.

4.2 Conclusions and future work

Gaining a clear picture of the mechanism driving cerebral reorganization for a particular individual's pattern of brain injury will enable the development of biomarkers for more accurate prognoses and development of personalized treatment plans using a Precision Medicine framework (Collins and Varmus, 2015). These personalized treatments could be based on cognitive or physical therapeutic approaches, or they could be physiological, e.g. non-invasive brain stimulation. Non-invasive brain stimulation has been shown to modify the brain's FC networks to boost recovery from stroke, depression and mild TBI (Demirtas-Tatlidede *et al.*, 2013; Grefkes and Fink, 2011). It is not clear how neuromodulation techniques influence the brain, but increases in FC between regions have been shown in high-frequency repetitive transcranial magnetic stimulation (rTMS) (Thut and Pascual-Leone, 2010). Currently, the choice of targets for brain stimulation is not well defined; many times it depends on population-level observations. If we can fully understand the mechanism of post-injury cerebral organization in terms of the structural and functional connectome relationship, then we may be able to identify region-pairs in a particular individual that, if functionally connected, would have the largest influence on improvements in attention and memory. We would be able to explicitly identify structural

pathways that could be used to establish this functional connection. Such regions and pathways would then be optimal targets for rTMS. This method for personalized target selection could be applied in a variety of neurological disorders, improving recovery and quality of life for patients with a range of neurological diseases.

Fig. Legends

Fig. 1: Functional rerouting/reconnection hypothesis The functional rerouting and/or reconnection hypothesis as a possible recovery mechanism after mild TBI.

Fig. 2: PCA coefficients of overall recovery The coefficients of the first component of the PCA analysis using 27 subjects' data from one and 6 months. ANT scores are on the left and CVLT-II scores are on the right. Red indicates that sub-score's values are smaller = better and blue indicates that sub-score's values are higher = better.

Fig. 3: Longitudinal improvement in overall cognition The violin plots describe the overall cognitive scores (first PCA component) at 1 months and 6 months, with lines indicating individuals (N = 27). Individuals with increases in cognition from 1 month to 6 months are plotted in green, solid lines while decreases in cognition are plotted in red, dashed lines. *Significant improvement in overall cognitive scores from 1 month to 6 months ($p<0.05$).

Fig. 4: PLSR model of change in overall cognition Observed versus predicted change in overall cognition post-mild TBI. The corresponding R^2 is reported in the upper left corner.

Fig. 5: PLSR model coefficients Violin plots indicating the shape of the distribution of coefficients over the 26 leave-one-out PLSR models predicting overall cognitive recovery post-mild TBI from changes in various FC and SC global network metrics. Red lines indicate the median while the blue lines indicate the mean. Regression coefficients were considered important if their 95% CI did not contain zero in a majority of the 26 leave-one-out models (blue = important/positive, red = important/negative, black = not important).

Acknowledgements

None

Funding

This work was supported by an Anna-Maria and Stephen Kellen Foundation Junior Faculty Fellowship (AK) and the NIH [R01 NS060776 (PM), R21 NS104634-01 (AK), R01 NS102646-01A1 (AK)]. The authors have no conflicts of interest to disclose.

References

Abdelnour F, Voss HU, Raj A. Network diffusion accurately models the relationship between structural and functional brain connectivity networks. Neuroimage 2014; 90: 335–47.

Ashman TA, Gordon WA, Cantor JB, Hibbard MR. Neurobehavioral consequences of traumatic brain injury. Mt. Sinai J. Med. 2006; 73: 999–1005.

Behzadi Y, Restom K, Liau J, Liu TT. A component based noise correction method (CompCor) for BOLD and perfusion based fMRI. Neuroimage 2007; 37: 90–101.

Benjamini Y, Hochberg Y. Controlling the false discovery rate: a practical and powerful approach to multiple testing. J. Roy. Stat. Soc. Ser. B 1995; 57: 289–300.

Bonnelle V, Leech R, Kinnunen KM, Ham TE, Beckmann CF, De Boissezon X, et al. Default mode network connectivity predicts sustained attention deficits after traumatic brain injury. J. Neurosci. 2011; 31: 13442–51.

Brenner LA. Neuropsychological and neuroimaging findings in traumatic brain injury and post-traumatic stress disorder. Dialogues Clin. Neurosci. 2011; 13: 311–323.

Cabral J, Hugues E, Sporns O, Deco G. Role of local network oscillations in resting-state functional connectivity. Neuroimage 2011; 57: 130–9.

Caeyenberghs K, Leemans A, Leunissen I, Gooijers J, Michiels K, Sunaert S, et al. Altered structural networks and executive deficits in traumatic brain injury patients. Brain Struct. Funct. 2014; 219: 193–209.

Caeyenberghs K, Leemans A, Leunissen I, Michiels K, Swinnen SP. Topological correlations of structural and functional networks in patients with traumatic brain injury. Front. Hum. Neurosci. 2013; 7: 726.

Caeyenberghs K, Verhelst H, Clemente A, Wilson PH. Mapping the functional connectome in traumatic brain injury: What can graph metrics tell us? Neuroimage 2017; 160: 113–123.

Chai XJ, Castañón AN, Ongür D, Whitfield-Gabrieli S. Anticorrelations in resting state networks without global signal regression. Neuroimage 2012; 59: 1420–8.

Collins FS, Varmus H. A New Initiative on Precision Medicine. N. Engl. J. Med. 2015; 372: 793–795.

Das TK, Abeyasinghe PM, Crone JS, Sosnowski A, Laureys S, Owen AM, et al. Highlighting the Structure-Function Relationship of the Brain with the Ising Model and Graph Theory. Biomed. Res. Int. 2014; 4: 237898.

Deco G, Senden M, Jirsa V. How anatomy shapes dynamics: a semi-analytical study of the brain at rest by a simple spin model. Front. Comput. Neurosci. 2012; 6: 68.

Demertzi A, Gómez F, Crone JS, Vanhaudenhuyse A, Tshibanda L, Noirhomme Q, et al. Multiple fMRI system-level baseline connectivity is disrupted in patients with consciousness alterations. Cortex. 2014; 52: 35–46.

Demirtas-Tatlidede A, Vahabzadeh-Hagh AM, Bernabeu M, Tormos JM, Pascual-Leone A. Noninvasive brain stimulation in traumatic brain injury. J. Head Trauma Rehabil. 2013; 27: 274–92.

Dinkel J, Drier A, Khalilzadeh O, Perlbarg V, Czernecki V, Gupta R, et al. Long-term white matter changes after severe traumatic brain injury: a 5-year prospective cohort. AJNR. Am. J. Neuroradiol. 2014; 35: 23–9.

Efron B. Better Bootstrap Confidence Intervals. J. Am. Stat. Assoc. 1987; 82: 171–185.

Fan J, McCandliss BD, Sommer T, Raz A, Posner MI. Testing the efficiency and

independence of attentional networks. J. Cogn. Neurosci. 2002; 14: 340–7.

Fernández-Espejo D, Bekinschtein T, Monti MM, Pickard JD, Junque C, Coleman MR, et al. Diffusion weighted imaging distinguishes the vegetative state from the minimally conscious state. Neuroimage 2011; 54: 103–12.

Fernández Galán R. On how network architecture determines the dominant patterns of spontaneous neural activity. PLoS One 2008; 3: e2148.

Fischl B, Dale AM. Measuring the thickness of the human cerebral cortex from magnetic resonance images. Proc. Natl. Acad. Sci. U. S. A. 2000; 97: 11050–5.

Grefkes C, Fink GR. Reorganization of cerebral networks after stroke: new insights from neuroimaging with connectivity approaches. Brain 2011; 134: 1264–76.

Hampson M, Driesen NR, Skudlarski P, Gore JC, Constable RT. Brain connectivity related to working memory performance. J. Neurosci. 2006; 26: 13338–43.

Hillary FG, Rajtmajer SM, Roman CA, Medaglia JD, Slocomb-Dluzen JE, Calhoun VD, et al. The rich get richer: Brain injury elicits hyperconnectivity in core subnetworks. PLoS One 2014; 9

Honey CJ, Sporns O, Cammoun L, Gigandet X, Thiran JP, Meuli R, et al. Predicting human resting-state functional connectivity from structural connectivity. Proc. Natl. Acad. Sci. U. S. A. 2009; 106: 2035–40.

van der Horn HJ, Kok JG, de Koning ME, Scheenen ME, Leemans A, Spikman JM, et al. Altered Wiring of the Human Structural Connectome in Adults with Mild Traumatic Brain Injury. J. Neurotrauma 2017; 34: 1035–1044.

van der Horn HJ, Liemburg EJ, Scheenen ME, de Koning ME, Spikman JM, van der Naalt J. Graph Analysis of Functional Brain Networks in Patients with Mild Traumatic

Brain Injury. PLoS One 2017; 12: e0171031.

Hukkelhoven CWPM, Steyerberg EW, Rampen AJJ, Farace E, Habbema JDF, Marshall LF, et al. Patient age and outcome following severe traumatic brain injury: an analysis of 5600 patients. J. Neurosurg. 2003; 99: 666–673.

Irimia A, Wang B, Aylward SR, Prastawa MW, Pace DF, Gerig G, et al. Neuroimaging of structural pathology and connectomics in traumatic brain injury: Toward personalized outcome prediction. NeuroImage. Clin. 2012; 1: 1–17.

Jacobs ML, Donders J. Criterion validity of the California Verbal Learning Test-Second Edition (CVLT-II) after traumatic brain injury. Arch. Clin. Neuropsychol. 2007; 22: 143–9.

Kim J, Parker D, Whyte J, Hart T, Pluta J, Ingalhalikar M, et al. Disrupted Structural Connectome Is Associated with Both Psychometric and Real-World Neuropsychological Impairment in Diffuse Traumatic Brain Injury. J. Int. Neuropsychol. Soc. 2014; 20: 887–896.

Krishnan A, Williams LJ, McIntosh AR, Abdi H. Partial Least Squares (PLS) methods for neuroimaging: a tutorial and review. Neuroimage 2011; 56: 455–75.

Kuceyeski A, Maruta J, Niogi SN, Ghajar J, Raj A. The generation and validation of white matter connectivity importance maps. Neuroimage 2011; 58: 109–21.

Kuceyeski A, Shah S, Dyke JP, Bickel S, Abdelnour F, Schiff ND, et al. The application of a mathematical model linking structural and functional connectomes in severe brain injury. NeuroImage Clin. 2016; 11: 635–647.

Langlois JA, Rutland-Brown W, Wald MM. The epidemiology and impact of traumatic brain injury: a brief overview. J. Head Trauma Rehabil. 2006; 21: 375–8.

Laureys S, Schiff ND. Coma and consciousness: paradigms (re)framed by neuroimaging. Neuroimage 2012; 61: 478–91.

Losoi H, Silverberg ND, Wäljas M, Turunen S, Rosti-Otajärvi E, Helminen M, et al. Recovery from Mild Traumatic Brain Injury in Previously Healthy Adults. J. Neurotrauma 2016; 33: 766–776.

Marquez de la Plata CD, Hart T, Hammond FM, Frol AB, Hudak A, Harper CR, et al. Impact of age on long-term recovery from traumatic brain injury. Arch. Phys. Med. Rehabil. 2008; 89: 896–903.

McAllister TW, Flashman LA, McDonald BC, Saykin AJ. Mechanisms of working memory dysfunction after mild and moderate TBI: evidence from functional MRI and neurogenetics. J. Neurotrauma 2006; 23: 1450–67.

McCrea M, Iverson GL, McAllister TW, Hammeke TA, Powell MR, Barr WB, et al. An integrated review of recovery after mild traumatic brain injury (MTBI): implications for clinical management. Clin. Neuropsychol. 2009; 23: 1368–90.

Messé A, Rudrauf D, Benali H, Marrelec G. Relating structure and function in the human brain: relative contributions of anatomy, stationary dynamics, and non-stationarities. PLoS Comput. Biol. 2014; 10: e1003530.

Nakamura T, Hillary FG, Biswal BB. Resting network plasticity following brain injury. PLoS One 2009; 4: e8220.

Niogi SN, Mukherjee P, Ghajar J, Johnson C, Kolster RA, Sarkar R, et al. Extent of microstructural white matter injury in postconcussive syndrome correlates with impaired cognitive reaction time: a 3T diffusion tensor imaging study of mild traumatic brain injury. AJNR. Am. J. Neuroradiol. 2008; 29: 967–73.

Palacios EM, Sala-Llonch R, Junque C, Roig T, Tormos JM, Bargallo N, et al. Resting-state functional magnetic resonance imaging activity and connectivity and cognitive outcome in traumatic brain injury. JAMA Neurol. 2013; 70: 845–51.

Pandit AS, Expert P, Lambiotte R, Bonnelle V, Leech R, Turkheimer FE, et al. Traumatic brain injury impairs small-world topology. Neurology 2013; 80: 1826–33.

Rubinov M, Sporns O. Complex network measures of brain connectivity: uses and interpretations. Neuroimage 2010; 52: 1059–69.

Sharp DJ, Beckmann CF, Greenwood R, Kinnunen KM, Bonnelle V, De Boissezon X, et al. Default mode network functional and structural connectivity after traumatic brain injury. Brain 2011; 134: 2233–47.

Sharp DJ, Scott G, Leech R. Network dysfunction after traumatic brain injury. Nat. Rev. Neurol. 2014; 10: 156–66.

Sidaros A, Engberg AW, Sidaros K, Liptrot MG, Herning M, Petersen P, et al. Diffusion tensor imaging during recovery from severe traumatic brain injury and relation to clinical outcome: a longitudinal study. Brain 2008; 131: 559–72.

Soddu A, Vanhaudenhuyse A, Demertzi A, Bruno M-A, Tshibanda L, Di H, et al. Resting state activity in patients with disorders of consciousness. Funct. Neurol. 2011; 26: 37–43.

Spielberg JM, McGlinchey RE, Milberg WP, Salat DH. Brain Network Disturbance Related to Posttraumatic Stress and Traumatic Brain Injury in Veterans. Biol. Psychiatry 2015; 78: 210–216.

Thut G, Pascual-Leone A. A review of combined TMS-EEG studies to characterize lasting effects of repetitive TMS and assess their usefulness in cognitive and clinical

neuroscience. Brain Topogr. 2010; 22: 219–32.

Vanhaudenhuyse A, Noirhomme Q, Tshibanda LJ-F, Bruno M-A, Boveroux P, Schnakers C, et al. Default network connectivity reflects the level of consciousness in non-communicative brain-damaged patients. Brain 2010; 133: 161–71.

Voss HU, Uluç AM, Dyke JP, Watts R, Kobylarz EJ, McCandliss BD, et al. Possible axonal regrowth in late recovery from the minimally conscious state. J. Clin. Invest. 2006; 116: 2005–11.

Whitfield-Gabrieli S, Nieto-Castanon A. Conn: a functional connectivity toolbox for correlated and anticorrelated brain networks. Brain Connect. 2012; 2: 125–41.

Willmott C, Ponsford J, Hocking C, Schönberger M. Factors contributing to attentional impairments after traumatic brain injury. Neuropsychology 2009; 23: 424–432.

Wood RL. Understanding the 'miserable minority': a diasthesis-stress paradigm for post-concussional syndrome. Brain Inj. 2004; 18: 1135–53.

Woolrich MW, Stephan KE. Biophysical network models and the human connectome. Neuroimage 2013; 80: 330–8.

Yuh EL, Cooper SR, Mukherjee P, Yue JK, Lingsma HF, Gordon WA, et al. Diffusion tensor imaging for outcome prediction in mild traumatic brain injury: a TRACK-TBI study. J. Neurotrauma 2014; 31: 1457–77.

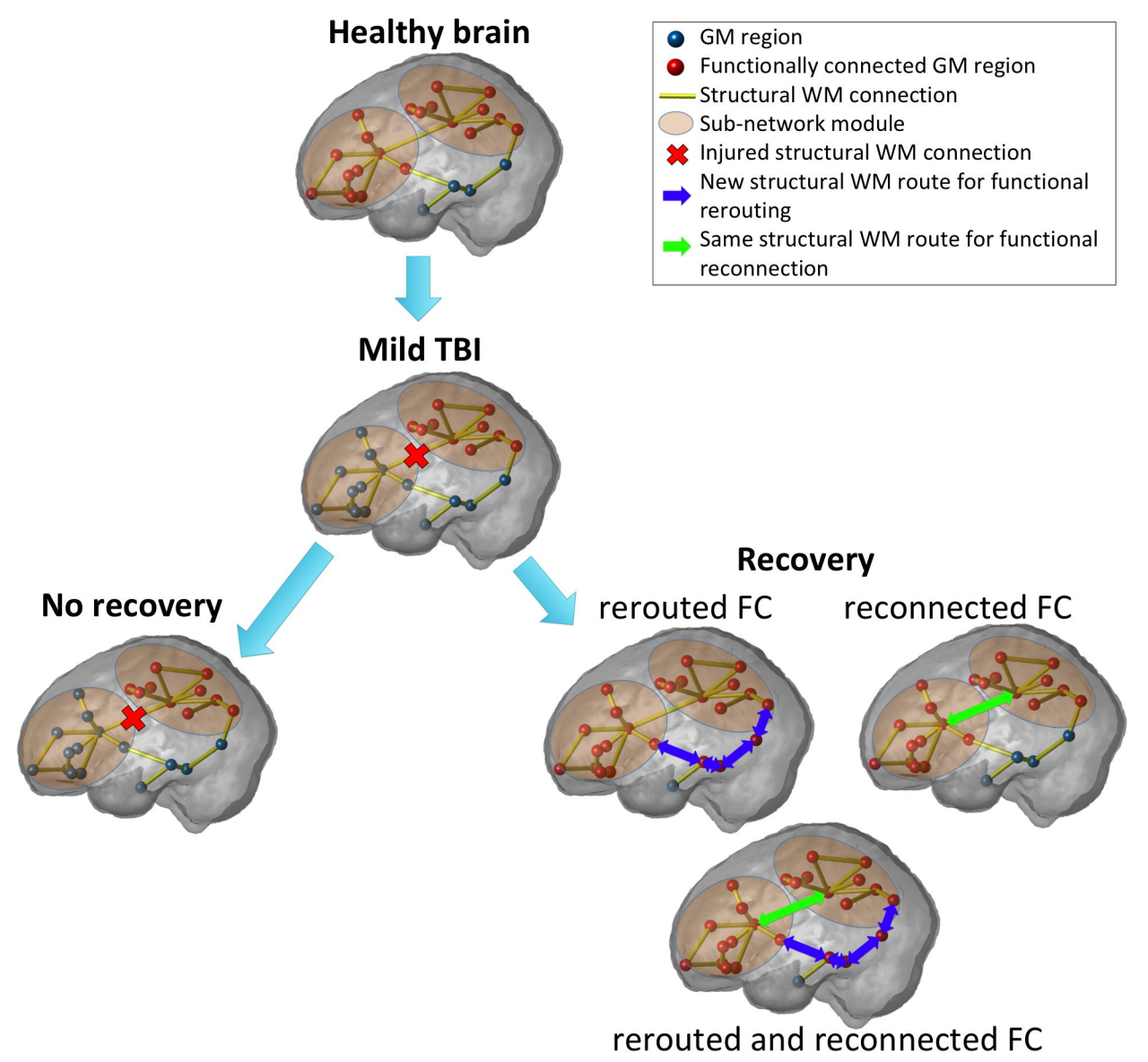
Healthy brain
GM region
Functionally connected GM region
Structural WM connection
Sub-network module
Injured structural WM connection
New structural WM route for functional rerouting
Same structural WM route for functional reconnection
Mild TBI
No recovery
Recovery
rerouted FC
reconnected FC
rerouted and reconnected FC

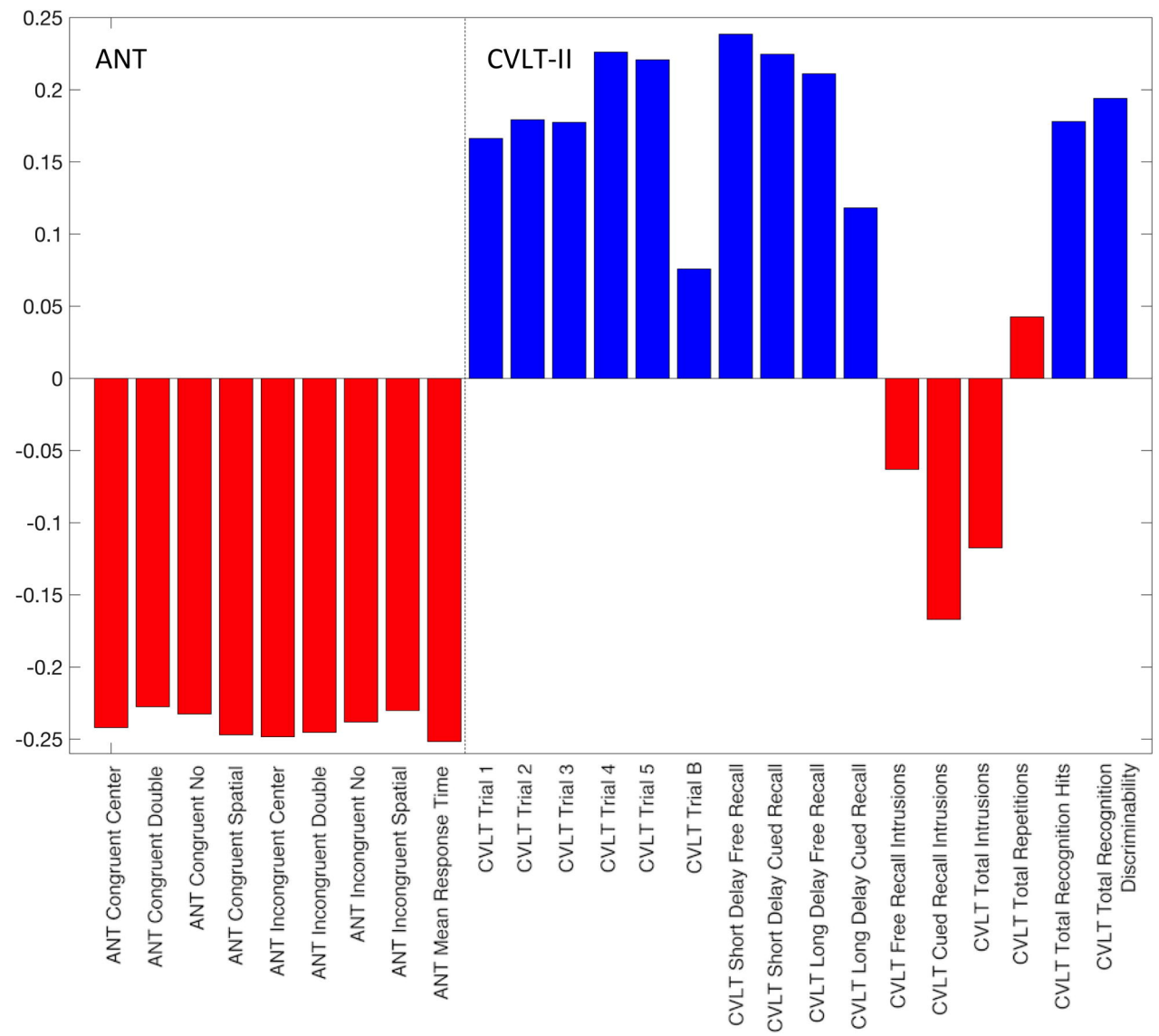
ANT
CVLT-II
0.25
0.2
0.15
0.1
0.05
0
-0.05
-0.1
-0.15
-0.2
-0.25
ANT Congruent Center
ANT Congruent Double
ANT Congruent No
ANT Congruent Spatial
ANT Incongruent Center
ANT Incongruent Double
ANT Incongruent No
ANT Incongruent Spatial
ANT Mean Response Time
CVLT Trial 1
CVLT Trial 2
CVLT Trial 3
CVLT Trial 4
CVLT Trial 5
CVLT Trial B
CVLT Short Delay Free Recall
CVLT Short Delay Cued Recall
CVLT Long Delay Free Recall
CVLT Long Delay Cued Recall
CVLT Free Recall Intrusions
CVLT Cued Recall Intrusions
CVLT Total Intrusions
CVLT Total Repetitions
CVLT Total Recognition Hits
CVLT Total Recognition Discriminability

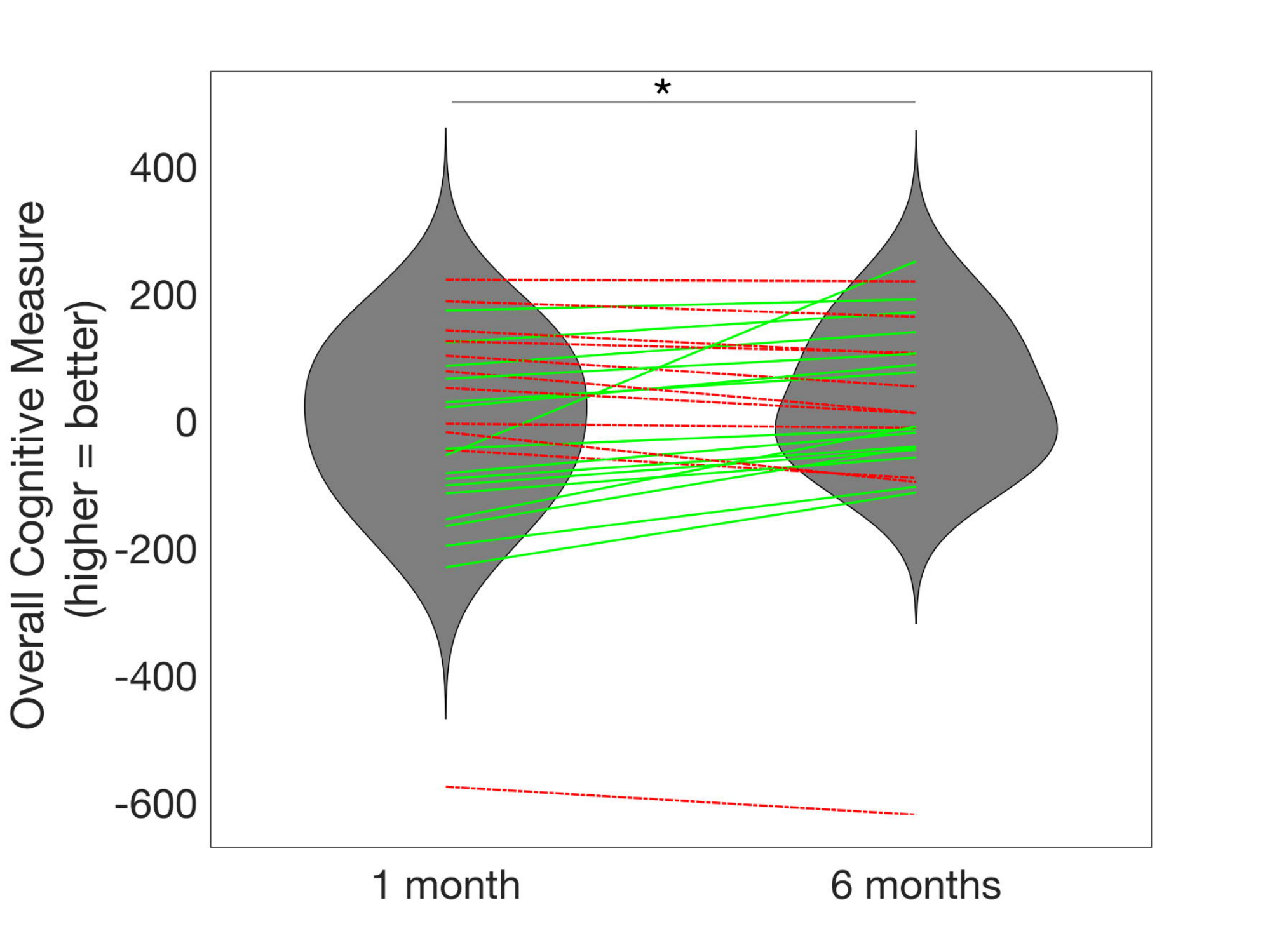
*
400
200
0
-200
-400
-600
Overall Cognitive Measure
(higher = better)
1 month
6 months

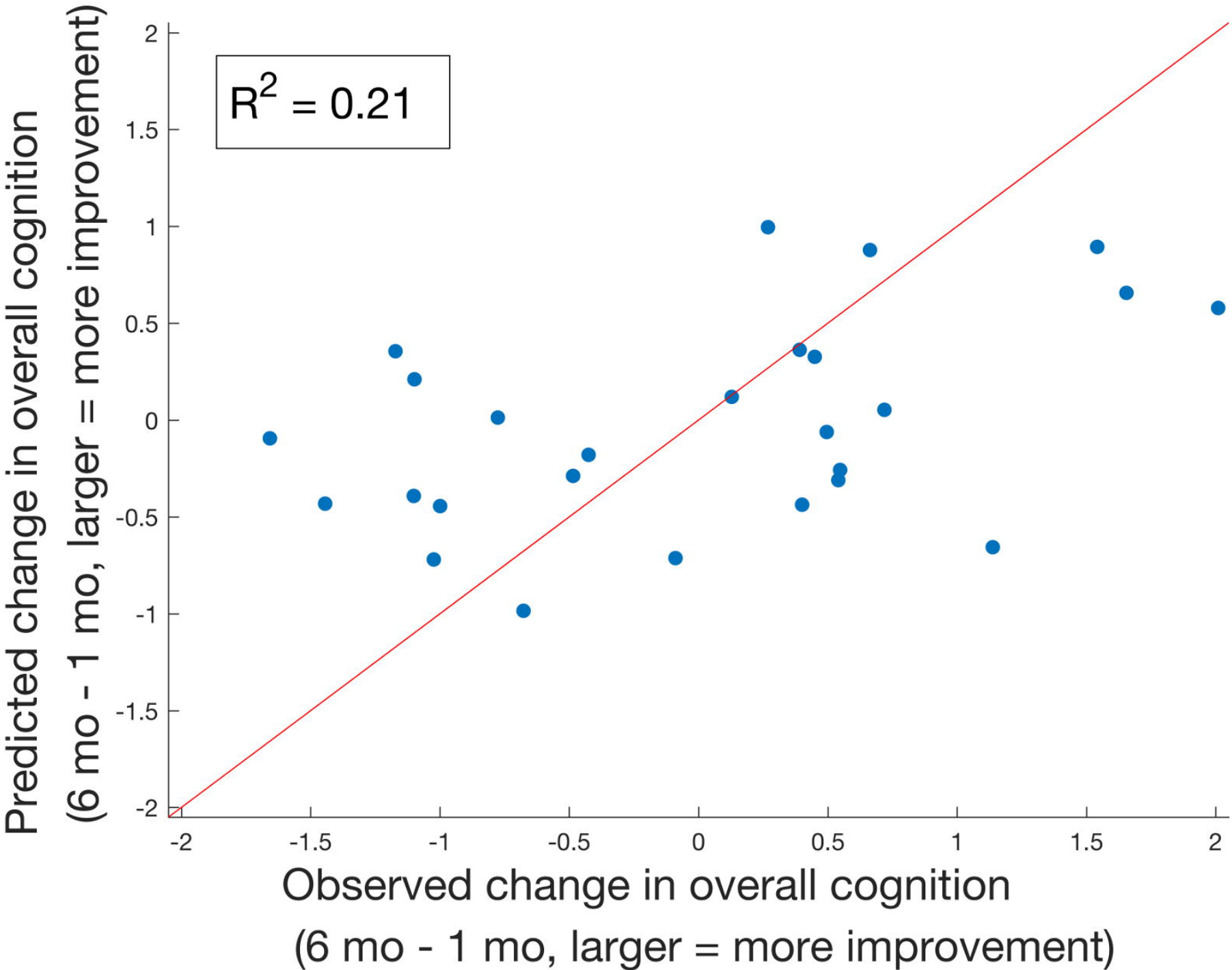
R^2 = 0.21
Predicted change in overall cognition
(6 mo - 1 mo, larger = more improvement)
Observed change in overall cognition
(6 mo - 1 mo, larger = more improvement)
2
1.5
1
0.5
0
-0.5
-1
-1.5
-2
-2
-1.5
-1
-0.5
0
0.5
1
1.5
2

Mean
Median
PLSR regression coefficient
0.2
0.15
0.1
0.05
0
-0.05
-0.1
-0.15
-0.2
ΔND propaga-tion time
ΔSC character-istic path length
ΔSC efficiency
ΔSC Small-worldness
ΔFC efficiency
ΔFC clustering coefficient
ΔFC modularity